Organic Electronics 14 (2013) 1086–1093

Contents lists available at SciVerse ScienceDirect

Organic Electronics

journal homepage: www.elsevier.com/locate/orgel

Fine-tuning the balance between carbazole and oxadiazole units in bipolar hosts to realize highly efficient green PhOLEDs

Shuo-Hsien Cheng [a], Shu-Hua Chou [a], Wen-Yi Hung [b,*], Hong-Wei You [b], You-Ming Chen [a], Atul Chaskar [a], Yi-Hung Liu [a], Ken-Tsung Wong [a,*]

[a] Department of Chemistry, National Taiwan University, Taipei 106, Taiwan
[b] Institute of Optoelectronic Sciences, National Taiwan Ocean University, Keelung 202, Taiwan

ARTICLE INFO

Article history:
Received 15 November 2012
Received in revised form 3 January 2013
Accepted 3 January 2013
Available online 8 February 2013

Keywords:
PhOLEDs
Bipolar host
Carbazole/oxadiazole

ABSTRACT

A series of new bipolar hosts **C1O1**, **C2O1**, and **C1O2** comprising hole-transporting carbazole as donor (D) and electron-transporting oxadiazole as acceptor (A) have been designed and synthesized to tune D/A ratio with a view for getting in-depth information about structure–property–performance relationship. The D/A ratio exerts subtle influences on absorption spectra and energy levels. Time-of-flight (TOF) measurements reveal that the increment of donor units effectively increase the hole mobility. The appropriate energy levels and triplet energies along with promising morphological and thermal stability of these molecules bring out them as suitable hosts to realize green PhOLEDs with $(PBi)_2Ir(acac)$ and $(PPy)_2Ir(acac)$ emitters. Green phosphorescent devices hosted by **C1O1**, **C2O1**, and **C1O2** achieved maximum external quantum efficiencies of 20.7%, 20.4%, and 17.3%, respectively. These results indicate that carbazole/oxadiazole hybrid molecule with one carbazole and oxadiazole each is a better candidate for highly efficient green PhOLEDs.

1. Introduction

Phosphorescent OLEDs (PhOLEDs), known for effectively utilizing both singlet and triplet excitons to achieve a 100% internal quantum efficiency (IQE), have received great research attentions both from academia and industrial [1,2]. To realize highly efficient electrophosphorescence, transition metal-based emitters are usually dispersed into a suitable host material for suppressing triplet–triplet annihilation and self-quenching of phosphors [3]. As host materials essentially manage both charge transport and recombination functions and also play a vital role to confine emissive excitons within the emitting layer, the molecular design of host material becomes a crucial issue. Efficient host materials should possess properties such as good morphological and thermal stability for retaining the amorphous thin film quality, balanced charge transport characters to afford sufficient charge flux, high triplet energy (E_T) for preventing exciton quenching, and suitable energy levels relative to the neighboring layers for giving low operation voltage [4]. The design of bipolar host materials configured with electron-donating structures as donors (D) and electron-deficient groups as acceptors (A) seems to be the most appealing strategy in recent years [5]. Among the hole-transporting components reported in the literature, carbazole has found and will continue to find extensive use in a myriad of material context for PhOLEDs due to their good hole-transporting ability and sufficiently high E_T [6]. On the other hand, 1,3,4-oxadiazole [7] and other electron-withdrawing groups such as phosphine oxide [8], triazine [9], and benzimidazole [10], have been utilized as efficient electron-transporting acceptors. Their low-lying LUMOs are well matched to the neighboring electron-transport layer (ETL), diminishing electron-injection barrier and effectively transporting electrons to emitting layer. Due to the intrinsic dual-transport property, hole and electron mobilities and even energy levels could

* Corresponding authors. Tel.: +886 02 24622192x6718; fax: +886 02 24634360.
E-mail addresses: wenhung@mail.ntou.edu.tw (W.-Y. Hung), kenwong@ntu.edu.tw (K.-T. Wong).

1566-1199/$ - see front matter © 2013 Elsevier B.V. All rights reserved.
http://dx.doi.org/10.1016/j.orgel.2013.01.010

be individually tuned via given different donor and acceptor in one bipolar host material [11]. In addition, the physical properties of bipolar host materials and eventually the performance of device adopting them are closely governed by the number of hole- (HT) and electron- (ET) transporting moieties and their linking topology. For example, Lee et al. reported a series of bipolar materials comprised of different numbers of carbazole and diphenylphosphine oxide [12] where the HOMO and the LUMO can be suitably tailored to align with their neighboring active layers. In addition, the charge mobilities of bipolar molecules evidently vary along with the D/A ratio. Consequently, under the same device structure, the host material with lower D/A ratio gave higher current density, which can be directly attributed to the better electron transport property and lower ETL/EML energy barrier [13]. Because the charge balance is highly related to the inherent carrier mobility of functional materials and the interfacial charge injection barriers, this result revealed a facile way to modulate and balance the charge fluxes, giving an excellent example of structure–property–performance relationship of bipolar host materials. Considering the promising physical properties and good performance of carbazole- and oxadiazole-containing OLED materials, we reported in this paper the synthesis, properties and device characteristics of a series of bipolar host materials **C1O1**, **C2O1**, and **C1O2** comprising of different combinations of D (carbazole) and A (oxadiazole). The energy levels as well as carrier mobility of the bipolar host materials can be manipulated through altering the D/A ratio, while maintaining sufficiently high E_T to confine emissive excitons within the emitting layer. The devices gave the maximum external quantum efficiency (η_{ext}) of 20.7%, 20.4%, and 17.2% as **C1O1**, **C2O1**, and **C1O2** were adopted as hosts for green phosphor $(PPy)_2Ir(acac)$, respectively. These results revealed that bipolar host **C1O1** containing equal number of HT and ET components gave the most efficient device due to better interfacial energy alignment and smaller charge injection barrier.

2. Results and discussions

2.1. Synthesis

Scheme 1 depicts the synthesis of the title compounds **C1O1**, **C2O1**, and **C1O2**. Starting from the CN-substituted carbazole derivatives **1** [14], **2** [15], and **3** [16], which were converted to their corresponding tetrazole intermediates **4**, **5**, and **6** in excellent yields by treating with NaN_3 and NH_4Cl. The tetrazoles were reacted with biphenyl acid chloride **7**, which was prepared from its corresponding acid [17], to give the desired bipolar host materials **C1O1**, **C2O1**, and **C1O2** with excellent isolated yields. Their structural identities and purities were confirmed by satisfactory spectroscopic data and elemental analysis (see Supporting information). The resulting bipolar molecules were configured with the electron-accepting oxadiazole group attaching to the C3 position of electron-donating carbazole group. In addition, the peripheral oxadiazole was capped by a phenyl group together with a bulky 4-*tert*-butylphenylene at the *ortho* position to bring in steric hindrance and highly twisted conformation for improving morphological stability.

2.2. Crystal structures

The molecular structures of **C1O1** and **C1O2** were unambiguously verified from single-crystal X-ray diffraction analysis (Fig. 1). The highly twisted manner between the 4-*tert*-butylphenyl group and end-capping phenyl group can be obviously observed with dihedral angles of 61.11° for **C1O1** (C21–C26–C27–C32) and 73.47° for **C1O2** (C13–C18–C19–C24). Therefore, the introduction of twisted phenyl rings as peripheral blocking groups can enhancing the morphological stability by efficiently preventing the molecules from stacking. In addition, the carbazole and oxadiazole moieties in these two materials are nearly coplanar as evidenced by the small dihedral angles of 2.31° for **C1O1** (C7–C2–C1–N1) and 4.90° for

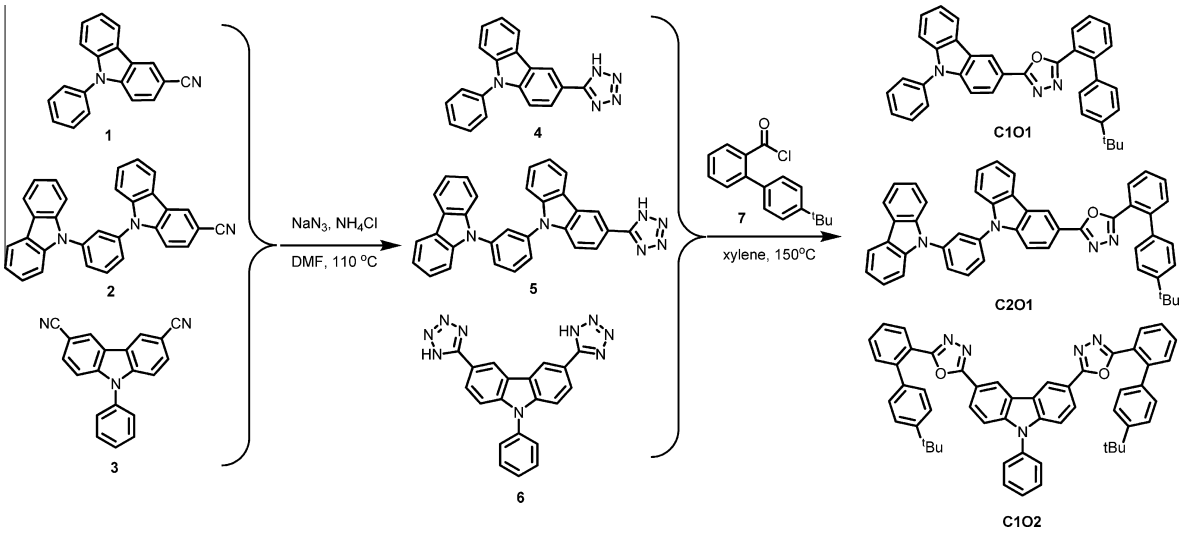

Scheme 1. Synthetic routes of **C1O1**, **C2O1**, and **C1O2**.

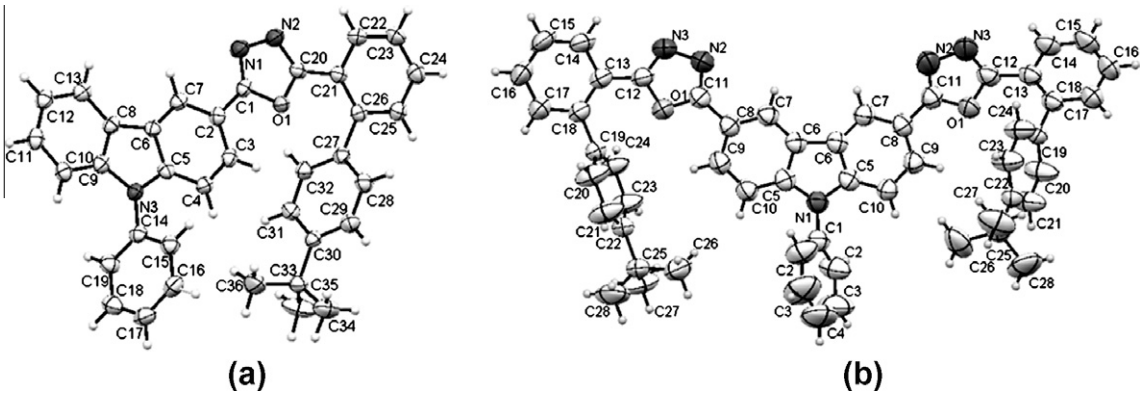

Fig. 1. ORTEP diagram of (a) **C1O1** and (b) **C1O2** with thermal ellipsoids shown at the 50% probability level.

C1O2 (C7–C8–C11–N2), indicating possible extended π-conjugation.

2.3. Thermal properties

The thermal stability and morphological property of **C1O1**, **C2O1**, and **C1O2** were determined by thermogravimetric analysis (TGA) and differential scanning calorimetry (DSC), respectively (Table 1). The decomposition temperatures (T_d), corresponding to 5% weight loss, were ranged in 320–400 °C, and the glass-transition temperature (T_g) were varied from 95 to 143 °C. It is clear that the thermal and morphological stability closely correlate to the molecular weights. The introduction of the *tert*-butylphenyl moiety greatly improves the T_d and T_g as compared to those of a bipolar molecule without such substitution reported previously [18]. As a result, these relatively high T_d together with high T_g highlight the suitability of these material to render high quality of amorphous thin film upon vacuum thermal evaporation, which is a desirable property for the material to be used in realization of highly efficient PhOLED as it suppresses the aggregates formation and imparts morphological stability.

2.4. Physical properties

Fig. 2 presents the UV–vis absorption and photoluminescence (PL) spectra of **C1O1**, **C2O1**, and **C1O2** in CH_2Cl_2 solution. All the molecules exhibit two distinct peaks in the absorption spectra, where the absorption peaks around 300 nm are attributed to the π–π* transition of the carbazole moiety [11g,19] and the neighboring longer wavelength peaks are assigned to be the π–π* transition of chromophores with extended π-conjugation in the presence of oxadiazole substitution(s). This assumption can be verified by the observation that the absorption maximum shifts successively with the increasing number of oxadiazole such as **C1O1** (322 nm), **C2O1** (323 nm), and **C1O2** (333 nm). The PL spectra of **C1O1** and **C2O1** centered around 400 nm were assigned to the intramolecular charge transfer (ICT) emission, which was confirmed by strong solvatochromic behavior in emission spectra (Fig. S1 in Supporting Information). Surprisingly, the emission spectrum of **C1O2** also centered at 400 nm, but performed relatively weak solvatochromism, indicating low charge-separated tendency in the excited state of **C1O2**. To shed light on the structure–property relationship, we performed theoretical calculations on the frontier molecular orbitals using density function theory (DFT) with 6-31G* basis sets (B3LYP/6-31G*) for the geometry optimization (Fig. 3). It is interesting to note that the HOMOs of **C1O1** and **C2O1** are mostly localized on the electron-donating carbazole center, whereas the LUMOs are shifted to the peripheral electron-accepting oxadiazole moieties, leading to an obvious spatial separation of frontier orbitals. This result fully agrees with the strong solvatochromism observed in **C1O1**. In contrast, the HOMO and LUMO of **C1O2** are effectively delocalized over the electron-donating and -accepting moieties, leading to a weak trend of charge transfer upon photo-excitation. These results support the observed red-shifted absorption and the absence of prominent solvatochromic effect in the emission spectra of **C1O2**. The neat film PL emissions of these molecules are red-shifted by 10–16 nm as compared to those in CH_2Cl_2 solution,

Table 1
Physical properties of **C1O1**, **C2O1**, and **C1O2**.

	$T_g/T_c/T_m$ (°C)	T_d (°C)	λ_{abs}, sol[a] (nm)	λ_{abs}, film (nm)	λ_{PL}, sol[a] (nm)	λ_{PL}, film (nm)	E_T[b] (eV)	HOMO/LUMO/E_g[c] (eV)
C1O1	95/–/–	322	300, 322	302, 329	393	403	2.52	5.55/2.24/3.31
C2O1	128/237/–	395	292, 323	295, 327	389	401	2.55	5.70/2.30/3.40
C1O2	143/212/273	399	305, 333	307, 337	384	400	2.50	5.50/2.15/3.35

[a] Measured in CH_2Cl_2.
[b] Measured in EtOH at 77 K.
[c] HOMO energy level determined by using photoelectron yield spectroscopy (AC-2). LUMO = HOMO + Eg, where Eg is calculated from the absorption onset of film state.

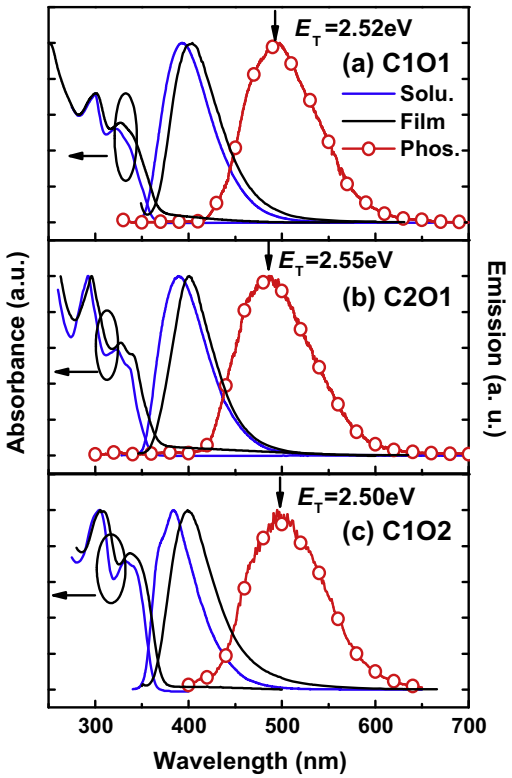

Fig. 2. Room-temperature absorption and emission (PL) spectra of **C1O1**, **C2O1**, and **C1O2** in the form of solution and neat films and corresponding phosphorescence (Phos.) spectra recorded from their EtOH solutions at 77 K.

which is typically encountered in bipolar organic materials [20]. The triplet energies (E_T) of **C1O1**, **C2O1**, and **C1O2** were determined to be 2.52, 2.55, and 2.50 eV, respectively, from the highest peak as the vibronic 0–0 transition of $T_1 \rightarrow S_0$ in the phosphorescence spectra acquired at 77 K in EtOH. Therefore, these materials should have sufficiently high triplet energies for hosting various green phosphorescent emitters.

Cyclic voltammetry (CV) was performed to probe the electrochemical property of **C1O1**, **C2O1**, and **C1O2** (Fig. S2 and Table S2). As referred to the redox couple of ferrocene/ferrocenium, the HOMO and LUMO energy levels of **C1O1**, **C2O1**, and **C1O2**, derived from the onsets of anodic and cathodic peaks, were estimated to be −5.74/−2.32, −5.67/−2.28, and −5.82/−2.30 eV with respect to the vacuum level respectively. According to the theoretical analysis, we assigned the reduction would occur on the oxadiazole center, giving **C1O1**, **C2O1**, and **C1O2** similar reduction potentials. Whereas, the oxidation center is localized on the carbazole core, which would be slightly affected by the number of acceptor groups as indicated that the HOMOs of **C1O1** and **C1O2** are −5.74 and −5.82 V, respectively. **C2O1** was found to have the lowest HOMO of −5.67 V, which is localized on the unsubstituted carbazole. For a more practical use, the HOMO levels of **C1O1**, **C2O1**, and **C1O2** in thin film were determined from the photoelectron yield spectroscopy (Riken AC-2), and the LUMO levels were calculated from the equation of LUMO = HOMO + E_g, where E_g is the optical band gap determined from the onset wavelength of thin-film absorption spectra. The HOMO/LUMO energy levels of **C1O1**, **C2O1**, and **C1O2** obtained by AC-2 are summarized in Table 1.

2.5. Carrier-transport properties

To further understand the charge-carrier transport properties of **C1O1**, **C2O1**, and **C1O2**, we used the time-of-flight (TOF) technique to evaluate the carrier mobilities [21]. Fig. 4a–c displays representative TOF transient for holes. The transit time, t_T, can be evaluated from the intersection point of two asymptotes in the double-logarithmic representation of the TOF transient. It is then used to determine the carrier mobilities, according to the equation $\mu = d^2/Vt_T$, where d is the sample thickness and V is the applied voltage. Fig. 4d reveals that the field dependence of the hole mobility follows the nearly universal Poole–Frenkel relationship, with values in the range from 2×10^{-5} to 8×10^{-7} $cm^2\ V^{-1}\ s^{-1}$. The bipolar molecule **C2O1** containing one free-substituted carbazole unit exhibits much higher hole mobility as compared to those of bipolar molecules with oxadiazole-substituted carbazole (**C1O1** and **C1O2**), where the hole mobilities are in the same order of magnitude. In contrast, the transient photocurrent signals for electrons were too weak for us to evaluate their mobilities using the TOF technique. Therefore, we fabricated electron-only devices having the device structure of ITO/BCP (30 nm)/compounds (50 nm)/TPBI (20 nm)/LiF/Al as shown in Fig. 5. Here, low-HOMO 2,9-dimethyl-4,7-diphenyl-1,10-phenanthroline (BCP, μ_e of 10^{-7} $cm^2\ V^{-1}\ s^{-1}$ order) [22] and 1,3,5-tris(*N*-phenylbenzimi-dazol-2-yl)benzene (TPBI, μ_e of 10^{-5} $cm^2\ V^{-1}s^{-1}$ order) [23] as the hole-blocking layer to impede the hole carriers in electron-only devices. In spite of the energy barriers in the ETL/Host interface, the similar *J–V* curves for these electron-only devices suggest that **C1O1**, **C2O1**, and **C1O2** have comparable electron-transport abilities. Based on these results we conclude that molecules **C1O1**, **C2O1**, and **C1O2** have bipolar transporting behavior.

2.6. OLED device

To investigate the new carbazole/oxadiazole hybrid materials (**C1O1**, **C2O1**, and **C1O2**) as hosts in organic light emitting diodes, we fabricated the emitting device with typical multi-layer architecture of indium–tin–oxide (ITO)/polyethylene dioxythiophene: polystyrene sulfonate (PEDOT:PSS, 30 nm)/1,1-bis[(di-4-tolylamino)phenyl]-9,9′-fluorene (DTAF, 25 nm)/emitter (25 nm)/1,3,5-tris(*N*-phenylbenzimidizol-2-yl)benzene (TPBI, 50 nm)/LiF (0.5 nm)/Al (100 nm). In view of the favorable triplet energy gaps of host (2.50–2.55 eV), we selected bis(2,*N*-diphenylbenzimidazolito)iridium(III) acetylacetonate $(PBi)_2Ir(acac)$ [24] and bis(2-phenylpyridinato) iridium(III) acetylacetonate $(PPy)_2Ir(acac)$ [2b] as green phosphors 10 wt% doped into the host as emissive layer. DTAF, with a high triplet level (E_T = 2.87 eV) and wide bandgap (E_g = 3.47 eV) can efficiently confine the triplet energy of phosphors, is selected as the hole-transporting layer

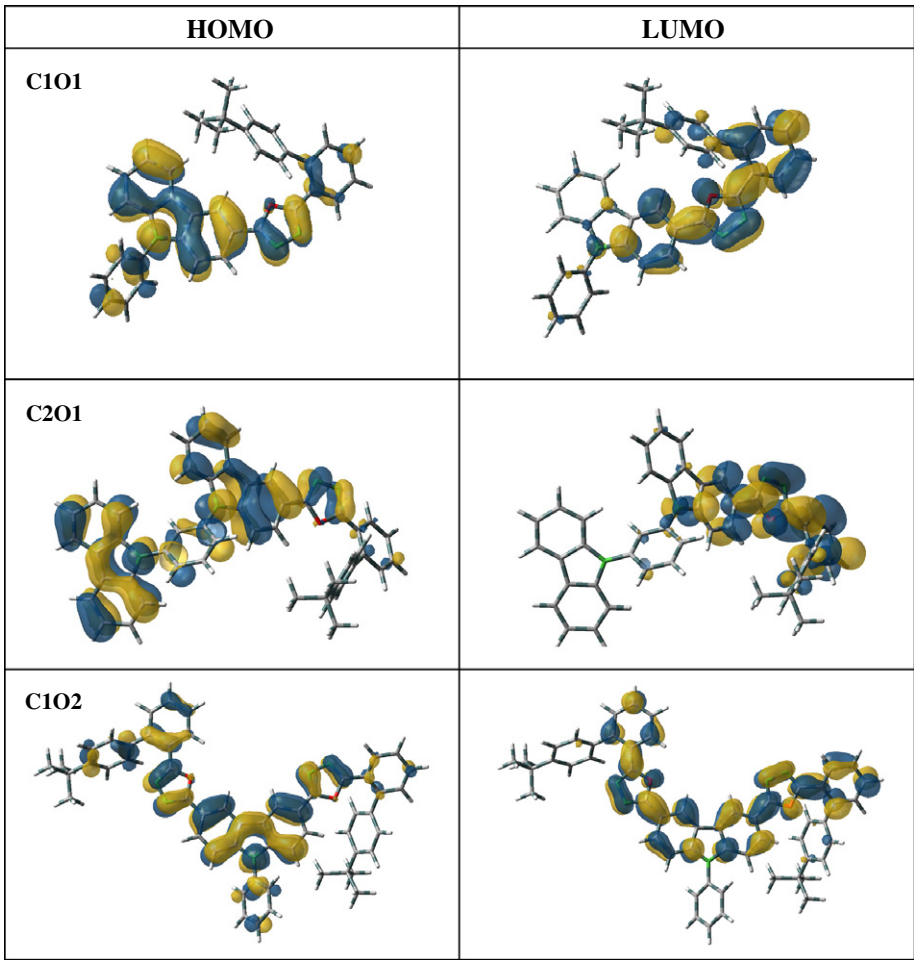

Fig. 3. Frontier molecular orbitals (HOMO and LUMO) of **C1O1**, **C2O1**, and **C1O2** calculated with DFT on a B3LYP/6-31G level.

(HTL) [25]. To further confine the holes or generated excitons within the emissive region, TPBI with a high-energy gap is selected as the electron-transporting layer (ETL) [11e]. PEDOT:PSS and LiF served as hole- and electron-injecting layer, respectively. Table 2 summarizes the EL characteristics of these PhOLEDs.

Fig. 6 presents the current density–voltage–luminance (*J*–*V*–*L*) characteristics, device efficiencies, and EL spectra of the devices incorporating **C1O1** (device A), **C2O1** (device B) and **C1O2** (device C). The notations 1 and 2 indicate the devices fabricated with green phosphors of $(PBi)_2Ir(acac)$ and $(PPy)_2Ir(acac)$, respectively. These devices exhibited turn-on voltages of 2.0 V (defined as the voltage at which EL became detectable) and maximum brightnesses of 104,000–144,000 cd m^{-2}. In devices A1 and A2, we employed **C1O1** as the host for $(PBi)_2Ir(acac)$ and $(PPy)_2Ir(acac)$, respectively. Device A2 had a maximum external quantum efficiency (η_{ext}) of 20.7%, which corresponds to current efficiency (η_c) of 77.1 cd A^{-1}. Due to the low operating voltages of device A2, its maximum power efficiency (η_p) reached 81 lm W^{-1}, and such high η_p is comparable with green PhOLEDs lacking a p–i–n junction [26]. When the brightness reached 1000 cd m^{-2}, the value of η_{ext} remained high (20%; retaining >96% of the external quantum efficiency), suggesting that balanced injection and transport of holes and electrons in the device occurred even at high current densities and reduce efficiency roll-off. For $(PBi)_2Ir(acac)$-based device A1, it also exhibited excellent device efficiencies (20.7%, 71.2 cd A^{-1}, 71 ml W^{-1}).

When compared with devices A1 and A2, devices B1 and B2 with **C2O1** as the host achieved similar device efficiencies (η_{ext} of 19.6–20.4%) as shown in Fig. 6b. However, only the device C based on **C1O2** reveals significantly lower device efficiencies (η_{ext} of 14.5–17.3%). This is consistent with the higher current density of **C1O2**-based device than those of the corresponding **C1O1**- and **C2O1**- based devices as shown in Fig. 6a. The energy barriers between the HOMOs of **C1O2** (−5.5 eV) and DTAF (−5.22 eV) are smaller than that of **C1O1** and **C2O1**. Therefore, holes can be easily injected into the EML, leading to unbalance holes and electrons in the emitting layer. In addition, the devices A and B incorporating **C1O1** and **C2O1** host exhibited higher efficiencies relative to those of device C incorporating **C1O2** as host, which may be due to the poor hole injection of devices A and B leading to the balanced carrier injection and transport in EMLs. We attributed this large

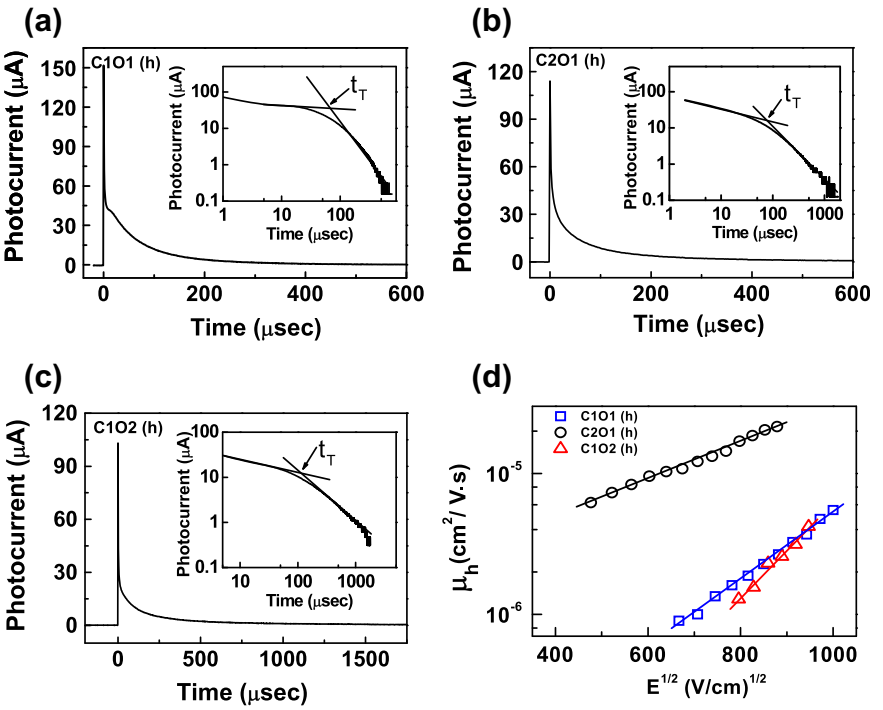

Fig. 4. Hole transient photocurrent signals for (a) **C1O1** (1.8 μm thick) at $E = 8.3 \times 10^5$ V/cm, (b) **C2O1** (2.2 μm thick) at $E = 4.1 \times 10^5$ V/cm, and (c) **C1O2** (1.9 μm thick) at $E = 8 \times 10^5$ V/cm. Insets are the double logarithmic plots of (a–c). (d) Hole mobilities of **C1O1**, **C2O1**, and **C1O2**, plotted with respect to $E^{1/2}$.

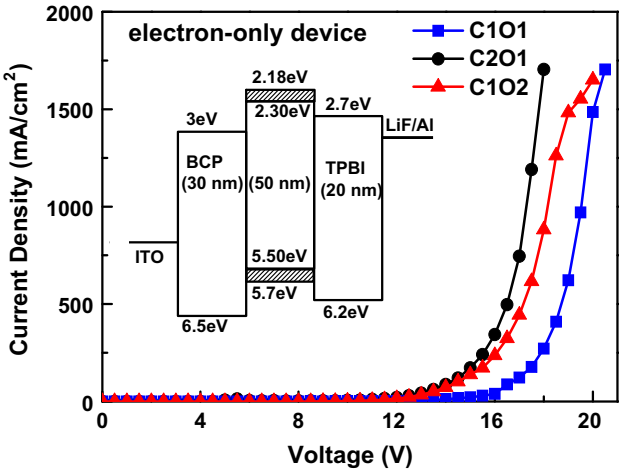

Fig. 5. Current density–voltage (*J*–*V*) characteristics of electron-only device.

Table 2
EL performance of devices as a function of the host and emitter.

	Host: 10% dopant	V_{on}[a] (V)	At 1000 nit[b] (V, %)	L_{max} (cd m^{-2})	I_{max} (mA cm^{-2})	η_{ext} (%)	η_c (cd A^{-1})	η_p (lm W^{-1})	CIE1931 (x, y)
A1	C1O1: $(PBi)_2Ir(acac)$	2	5.8, 20	127,000, 12.5	1180	20.7	71.2	71	0.39, 0.58
A2	C1O1: $(PPy)_2Ir(acac)$	2	5.7, 20	144,000, 11.5	1020	20.7	77.7	81	0.34, 0.62
B1	C2O1: $(PBi)_2Ir(acac)$	2	6, 19.5	162,000, 12.5	1460	20.4	66.4	66	0.39, 0.58
B2	C2O1: $(PPy)_2Ir(acac)$	2	6.2, 18	125,000, 12	1270	19.6	71.6	66.6	0.34, 0.62
C1	C1O2: $(PBi)_2Ir(acac)$	2	5.6, 16.8	104,000, 11.5	1270	17.3	58.4	61.5	0.38, 0.59
C2	C1O2: $(PPy)_2Ir(acac)$	2	5.2, 14.2	108,000, 11.5	1960	14.5	53.5	44.4	0.34, 0.62

[a] Turn-on voltage at which emission became detectable.
[b] The values of driving voltage and η_{ext} of device at 1000 cd m^{-2}.

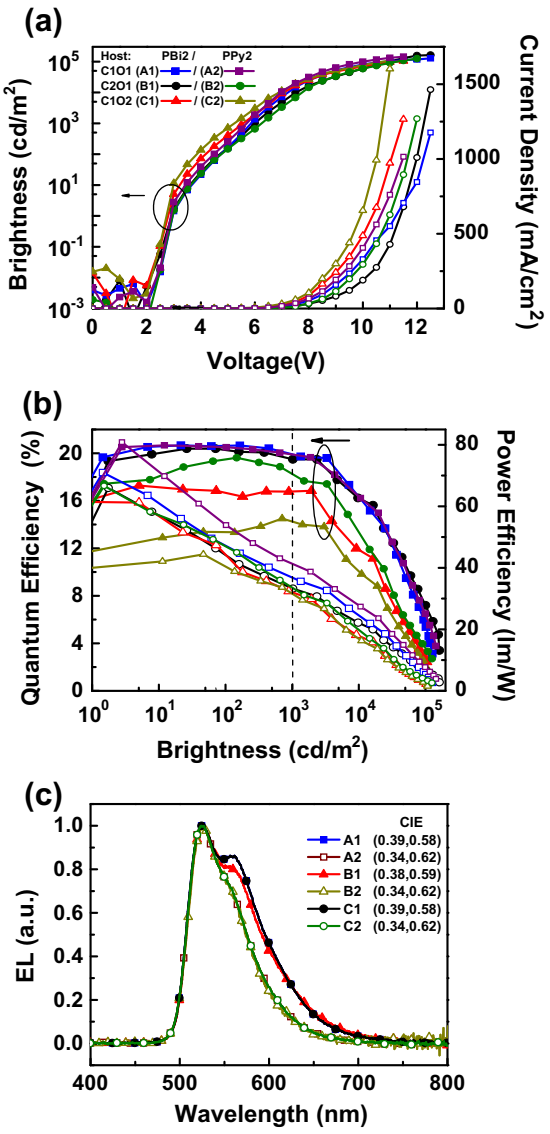

Fig. 6. (a) *J–V–L* characteristics, (b) plots of EL efficiency versus brightness and (c) EL spectra for devices incorporating host doped with 10 wt% $(PBi)_2Ir(acac)$ and $(PPy)_2Ir(acac)$.

enhancement in **C1O1**-based device performance to the well-matched energy levels, charge balance and triplet exciton confinement in the emitting layer.

3. Conclusions

In summary, we have synthesized three new bipolar hosts **C1O1**, **C2O1**, and **C1O2** featuring hole-transporting carbazole as donor core and electron-transporting oxadiazole peripheral. The carbazole/oxadiazole ratio exerts subtle influences on the physical properties such as thermal and morphological stability, absorption and emission, energy levels as well as hole mobility. Green PhOLEDs with maximum external quantum efficiency of 20.7%, 20.4%, and 17.3% has been achieved with $(PBi)_2Ir(acac)$ as emitter hosted by **C1O1**, **C2O1**, and **C1O2**, respectively. We accounted the best performance of **C1O1**-based device to the well matched energy levels and balanced charge flux along with effective exciton confinement. The molecular structure-physical property-EL performance relationship achieved in this work clearly indicates that varying the D to A ratio and linking topology could be a promising way to design new bipolar host materials for the realization of highly efficient PhOLEDs.

Acknowledgements

We are grateful to National Science Council (NSC 100-2112-M-019-002-MY3, 101-2119-M-002-007-MY3) and Ministry of Economic Affairs of Taiwan for financial support.

Appendix A. Supplementary material

Supplementary data associated with this article can be found, in the online version, at http://dx.doi.org/10.1016/j.orgel.2013.01.010.

References

[1] C.W. Tang, S.A. VanSlyke, Appl. Phys. Lett. 51 (1987) 913.
[2] (a) M.A. Baldo, D.F. O'Brien, Y. You, A. Shoustikov, S. Sibley, M.E. Thompson, S.R. Forrest, Nature 395 (1998) 151;
(b) C. Adachi, M.A. Baldo, M.E. Thompson, S.R. Forrest, J. Appl. Phys. 90 (2001) 5048.
[3] (a) M.A. Baldo, S. Lamansky, P.E. Burrows, M.E. Thompson, S.R. Forrest, Appl. Phys. Lett. 75 (1999) 4;
(b) S.-J. Su, H. Sasabe, T.I. Takeda, J. Kido, Chem. Mater. 20 (2008) 1691.
[4] (a) H.H. Fong, C.H. Wallace Choy, K.N. Hui, Y.J. Liang, App. Phys. Lett. 88 (2006) 113510;
(b) S.-y. Takizawa, V.A. Montes, P. Anzenbacher Jr., Chem. Mater. 21 (2009) 2452.
[5] (a) A. Chaskar, H.-F. Chen, K.-T. Wong, Adv. Mater. 23 (2011) 3876;
(b) Y. Tao, C. Yang, J. Qin, Chem. Soc. Rev. 40 (2011) 2943.
[6] (a) K.R.J. Thomas, J.T. Lin, Y.-T. Tao, C.-W. Ko, J. Am. Chem. Soc. 123 (2001) 9404;
(b) M.-H. Tsai, H.-W. Lin, H.-C. Su, T.-H. Ke, C.-C. Wu, F.-C. Fang, Y.-L. Liao, K.-T. Wong, C.-I. Wu, Adv. Mater. 18 (2006) 1216;
(c) S.-J. Su, C. Cai, J. Kido, Chem. Mater. 23 (2011) 274;
(d) D. Hu, F. Shen, H. Liu, P. Lu, Y. Lv, D. Liu, Y. Ma, Chem. Commun. 48 (2012) 3015;
(e) W. Jiang, Z. Ge, P. Cai, B. Huang, Y. Dai, Y. Sun, J. Qiao, L. Wang, L. Duan, Y. Qiu, J. Mater. Chem. 22 (2012) 12016.
[7] (a) M. Guan, Z. Chen, Z. Bian, Z. Liu, Z. Gong, W. Baik, H. Lee, C. Huang, Org. Electron. 7 (2006) 330;
(b) Y. Tao, Q. Wang, C. Yang, C. Zhong, K. Zhang, J. Qin, D. Ma, Adv. Funct. Mater. 20 (2010) 304;
(c) S. Gong, Y. Chen, J. Luo, C. Yang, C. Zhong, J. Qin, D. Ma, Adv. Funct. Mater. 21 (2011) 1168.
[8] (a) H.-H. Chou, C.-H. Cheng, Adv. Mater. 22 (2010) 2468;
(b) C. Fan, F. Zhao, P. Gan, S. Yang, T. Liu, C. Zhong, D. Ma, J. Qin, C. Yang, Chem. Eur. J. 18 (2012) 5510;
(c) S.O. Jeon, J.Y. Lee, J. Mater. Chem. 22 (2012) 4233.
[9] (a) H. Inomata, K. Goushi, T. Masuko, T. Konno, T. Imai, H. Sasabe, J.J. Brown, C. Adachi, Chem. Mater. 16 (2004) 1285;
(b) H.-F. Chen, S.-J. Yang, Z.-H. Tsai, W.-Y. Hung, T.-C. Wang, K.-T. Wong, J. Mater. Chem. 19 (2009) 8112.
[10] (a) Z. Ge, T. Hayakawa, S. Ando, M. Ueda, T. Akiike, H. Miyamoto, T. Kajita, M.-a. Kakimoto, Adv. Funct. Mater. 18 (2008) 584;
(b) C.-H. Chen, W.-S. Huang, M.-Y. Lai, W.-C. Tsao, J.T. Lin, Y.-H. Wu, T.-H. Ke, L.-Y. Chen, C.-C. Wu, Adv. Funct. Mater. 19 (2009) 2661.
[11] (a) Y.J. Shirota, Mater. Chem. 10 (2000) 1;
(b) R.J. Holmes, S.R. Forrest, Y.-J. Tung, R.C. Kwong, J.J. Brown, S. Garon, M.E. Thompson, Appl. Phys. Lett. 82 (2003) 2422;
(c) S. Tokito, T. Iijima, Y. Suzuri, H. Kita, T. Tsuzuki, F. Sato, Appl. Phys. Lett. 83 (2003) 569;

(d) K. Brunner, A.v. Dijken, H. Borner, J.J.A.M. Bastiaansen, N.M.M. Kiggen, B.M.W. Langeveld, J. Am. Chem. Soc. 126 (2004) 6035;
(e) S.-J. Yeh, M.-F. Wu, C.-T. Chen, Y.-H. Song, Y. Chi, M.-H. Ho, S.-F. Hsu, C.H. Chen, Adv. Mater. 17 (2005) 285;
(f) D. Tanaka, Y. Agata, T. Takeda, S. Watanabe, J. Kido, Jpn. J. Appl. Phys. 46 (2007) L117;
(g) M.-H. Tsai, T.-H. Ke, H.-W. Lin, C.-C. Wu, S.-F. Chiu, F.-C. Fang, Y.-L. Liao, K.-T. Wong, Y.-H. Chen, C.-I. Wu, ACS Appl. Mater. Interfaces 3 (2009) 567;
(h) H.-H. Chou, H.-H. Shih, C.-H. Cheng, J. Mater. Chem. 20 (2010) 798;
(i) Y. Tao, Q. Wang, C. Yang, C. Zhong, J. Qin, D. Ma, Adv. Funct. Mater. 20 (2010) 2923;
(j) W.-Y. Hung, L.-C. Chi, W.-J. Chen, Y.-M. Chen, S.-H. Chou, K.-T. Wong, J. Mater. Chem. 20 (2010) 10113.

[12] (a) S.O. Jeon, K.S. Yook, C.W. Joo, J.Y. Lee, Adv. Funct. Mater. 19 (2009) 3644;
(b) S.O. Jeon, S.E. Jang, H.S. Son, J.Y. Lee, Adv. Mater. 23 (2011) 1436.

[13] W. Jiang, L. Duan, J. Qiao, G. Dong, L. Wang, Y. Qiu, Org. Lett. 13 (2011) 3146.

[14] H. Mochizuki, T. Hasui, M. Kawamoto, T. Ikeda, C. Adachi, Y. Taniguchi, Y. Shirota, Macromolecules 36 (2003) 3457.

[15] M.-S. Lin, S.-J. Yang, H.-W. Chang, Y.-H. Huang, Y.-T. Tsai, C.-C. Wu, S.-H. Chou, E. Mondal, K.-T. Wong, J. Mater. Chem. 22 (2012) 16114.

[16] K.-J. Wei, J. Ni, J. Gao, Y. Liu, Q.-L. Liu, Eur. J. Inorg. Chem. (2007) 3868.

[17] C.B. Vu, J.C. Milne, D.P. Carney, J. Song, W. Choy, P.D. Lambert, D.J. Gagne, M. Hirsch, A. Cote, M. Davis, E. Lainez, N. Meade, K. Normington, M.R. Jirousek, R.B. Perni, Bioorg. Med. Chem. Lett. 19 (2009) 1416.

[18] H.-F. Chen, L.-C. Chi, W.-Y. Hung, W.-J. Chen, T.-Y. Hwu, Y.-H. Chen, S.-H. Chou, E. Mondal, Y.-H. Liu, K.-T. Wong, Org. Electron. 13 (2012) 2671.

[19] (a) S.-y. Takizawa, V.A. Montes, P. Anzenbacher Jr., Chem. Mater 21 (2009) 2452;
(b) W. Jiang, L. Duan, J. Qiao, G. Dong, D. Zhang, L. Wang, Y. Qiu, J. Mater. Chem. 21 (2011) 4918;
(c) Y. Ooyama, T. Sugiyama, Y. Oda, Y. Hagiwara, N. Yamaguchi, E. Miyazaki, H. Fukuoka, T. Mizumo, Y. Harima, J. Ohshita, Eur. J. Org. Chem. (2012) 4853;
(d) H.-p. Shi, J.-x. Dai, L.-w. Shi, L. Xu, Z.-b. Zhou, Y. Zhang, W. Zhou, C. Dong, Spectrochim. Acta Part A 93 (2012) 19;
(e) S.O. Jeon, J.Y. Lee, J. Mater. Chem. 22 (2012) 10537.

[20] (a) S. Shao, J. Ding, T. Ye, Z. Xie, L. Wang, X. Jing, F. Wang, Adv. Mater. 23 (2011) 3570;
(b) H.-F. Chen, T.-C. Wang, W.-Y. Hung, H.-C. Chiu, C. Yun, K.-T. Wong, J. Mater. Chem. 22 (2012) 9658;
(c) H. Huang, Y. Wang, S. Zhuang, X. Yang, L. Wang, C. Yang, J. Phys. Chem. C 116 (2012) 19458.

[21] P.M. Borsenberger, D.S. Weiss, Organic Photoreceptors for Imaging Systems, Marcel Dekker, New York, 1993.

[22] Z.-Y. Xie, T.-C. Wong, L.-S. Hung, S.-T. Lee, Appl. Phys. Lett. 80 (2002) 1477.

[23] W.-Y. Hung, T.-H. Ke, Y.-T. Lin, C.-C. Wu, T.-H. Hung, T.-C. Chao, K.-T. Wong, C.-I. Wu, Appl. Phys. Lett. 88 (2006) 064102.

[24] (a) W.-S. Huang, J.T. Lin, C.-H. Chien, Y.-T. Tao, S.-S. Sun, T.-S. Wen, Chem. Mater. 16 (2004) 2480;
(b) W.-S. Huang, J.T. Lin, H.-C. Lin, Org. Electron. 9 (2008) 557.

[25] (a) M.-T. Kao, W.-Y. Hung, Z.-H. Tsai, H.-W. You, H.-F. Chen, Y. Chi, K.-T. Wong, J. Mater. Chem. 21 (2011) 1846;
(b) W.-Y. Hung, H.-W. You, F.-C. Fan, H.-F. Chen, K.-T. Wong, Org. Electron. 12 (2011) 575.

[26] (a) Y. Tao, Q. Wang, C. Yang, Q. Wang, Z. Zhang, T. Zou, J. Qin, D. Ma, Angew. Chem. Int. Ed. 47 (2008) 8104;
(b) J. Zhao, G.-H. Xie, C.-R. Yin, L.-H. Xie, C.-M. Han, R.-F. Chen, H. Xu, M.-D. Yi, Z.-P. Deng, S.-F. Chen, Y. Zhao, S.-Y. g Liu, W. Huang, Chem. Mater. 23 (2011) 5331;
(c) C.-H. Chang, M.-C. Kuo, W.-C. Lin, Y.-T. Chen, K.-T. Wong, S.-H. Chou, E. Mondal, R.C. Kwong, S. Xia, T. Nakagawad, C. Adachi, J. Mater. Chem. 22 (2012) 3832.